Atmos. Meas. Tech., 6, 1095–1109, 2013
www.atmos-meas-tech.net/6/1095/2013/
doi:10.5194/amt-6-1095-2013

Atmospheric Measurement Techniques
Open Access

Development of a cavity-enhanced absorption spectrometer for airborne measurements of CH_4 and CO_2

S. J. O'Shea[1], S. J.-B. Bauguitte[2], M. W. Gallagher[1], D. Lowry[3], and C. J. Percival[1]

[1]School of Earth, Atmospheric and Environmental Sciences, University of Manchester, Oxford Road, Manchester, M13 9PL, UK
[2]Facility for Airborne Atmospheric Measurements (FAAM), Building 125, Cranfield University, Cranfield, Bedford, MK43 0AL, UK
[3]Department of Earth Sciences, Royal Holloway, University of London, Egham, UK

Correspondence to: S. J. O'Shea (sebastian.oshea@postgrad.manchester.ac.uk) and S. J.-B. Bauguitte (sbau@nerc.ac.uk)

Received: 26 November 2012 – Published in Atmos. Meas. Tech. Discuss.: 2 January 2013
Revised: 27 March 2013 – Accepted: 9 April 2013 – Published: 2 May 2013

Abstract. High-resolution CH_4 and CO_2 measurements were made on board the FAAM BAe-146 UK (Facility for Airborne Atmospheric Measurements, British Aerospace-146) atmospheric research aircraft during a number of field campaigns. The system was based on an infrared spectrometer using the cavity-enhanced absorption spectroscopy technique. Correction functions to convert the mole fractions retrieved from the spectroscopy to dry-air mole fractions were derived using laboratory experiments and over a 3 month period showed good stability. Long-term performance of the system was monitored using WMO (World Meteorological Office) traceable calibration gases. During the first year of operation (29 flights) analysis of the system's in-flight calibrations suggest that its measurements are accurate to 1.28 ppb (1σ repeatability at 1 Hz = 2.48 ppb) for CH_4 and 0.17 ppm (1σ repeatability at 1 Hz = 0.66 ppm) for CO_2. The system was found to be robust, no major motion or altitude dependency could be detected in the measurements. An inter-comparison between whole-air samples that were analysed post-flight for CH_4 and CO_2 by cavity ring-down spectroscopy showed a mean difference between the two techniques of -2.4 ppb ($1\sigma = 2.3$ ppb) for CH_4 and -0.22 ppm ($1\sigma = 0.45$ ppm) for CO_2. In September 2012, the system was used to sample biomass-burning plumes in Brazil as part of the SAMBBA project (South AMerican Biomass Burning Analysis). From these and simultaneous CO measurements, emission factors for savannah fires were calculated. These were found to be 2.2 ± 0.2 g (kg dry matter)$^{-1}$ for CH_4 and 1710 ± 171 g (kg dry matter)$^{-1}$ for CO_2, which are in excellent agreement with previous estimates in the literature.

1 Introduction

CO_2 and CH_4 are the 1st and 2nd most significant long lived greenhouse gases, respectively (Forster and Ramaswamy, 2007). Globally averaged CH_4 increased almost continuously from a pre-industrial level of ~ 700 to ~ 1800 ppb near the end of the 20th century (Etheridge et al., 1998). In more recent times the growth rate has been more changeable. Between 1990 and 2006 there was a general decline in the growth rate, but with increased year to year variations ranging from as high as 16.5 ± 0.9 ppb yr^{-1} in 1991 to as low as -3.8 ± 1.2 ppb yr^{-1} in 2004 (Simpson et al., 2006). Based on these previous observations it was suggested that a steady state had been reached, but the latest observations suggest that since 2007 the trend has increased once again (Rigby et al., 2008; Dlugokencky et al., 2009). A number of possible explanations for both the long-term and year to year variations have been suggested including: changes in global OH concentration, the major atmospheric sink for CH_4 (Dentener et al., 2003; Wang et al., 2004; Fiore et al., 2006); and changes in emissions from sources including rice agriculture, wetlands, biomass burning and the use of fossil fuels (Dlugokencky et al., 2001; Langenfelds et al., 2002; Simpson et al., 2006, 2012; Bousquet et al., 2011; Kai et al., 2011; Aydin et al., 2011; Levin et al., 2012). However, these changes are not yet fully understood nor unequivocally linked to the global trend in CH_4.

CO_2 mole fractions have also risen dramatically since pre-industrial times and are currently close to 400 ppm. This growth is widely attributed to anthropogenic activity (Forster

and Ramaswamy, 2007). Direct measurements of CO_2 have been made at the Manua Loa Observatory for nearly 50 years. From this remote background site along with the general growth a clear seasonal cycle can be identified, which is associated with varying fluxes from the Northern Hemisphere's biosphere. However, away from remote stations CO_2 levels reflect a myriad of competing source and sink processes (Lin et al., 2006).

The current network of ground-based greenhouse gas monitoring stations have proved sufficient to identify changes in the hemispheric and globally averaged mole fractions but have not been able to attribute changes to individual sources at regional scales. Such information is needed to confirm potential future feedbacks and for the mitigation of further growth (Marquis and Tans, 2008; Dlugokencky et al., 2011). Airborne measurements have been shown to be an increasingly powerful tool in assessing greenhouse gas budgets due to their ability to sample large spatial areas at high resolution (Pickett-Heaps et al., 2011; Patra et al., 2011; Wofsy et al., 2011; Baker et al., 2012); sample locations that cannot be easily accessed routinely by other methods (Kort et al., 2012); provide vertical concentration profiles, which are crucial for deriving accurate fluxes through inverse modelling (Stephens et al., 2007; Kort et al., 2011); and are a means to validate column-integrated measurements from remote sensing techniques (Washenfelder et al., 2006; Wunch et al., 2010; Deutscher et al., 2010; Wecht et al., 2012).

The World Meteorological Office (WMO) recommends an inter-laboratory comparability of ± 2 ppb for CH_4 and ± 0.1 ppm for CO_2 (WMO, 2007). Advancements in instrument technology to allow routine and rapid measurement of greenhouse gases to the necessary WMO specifications have been made for ground-based networks. However, operating such instruments on airborne platforms usually requires significant modification and understanding of environmental impacts on instrument performance and more frequent calibrations to meet these same specifications. For this reason, initially airborne measurements were generally made by collecting flask samples and analysing them on the ground (Keeling et al., 1968). Recently, spectroscopic techniques have become more robust and have started to be routinely deployed on airborne platforms due to their faster time response. These techniques include non-dispersive infrared absorption (NDIR), for the detection of CO_2 (Vay et al., 1999; Daube et al., 2002); and both direct laser absorption spectroscopy (Wofsy et al., 2011) and cavity ring-down spectroscopy (CRDS, Chen et al., 2010) for the detection of CO_2, CH_4 and other trace species.

This paper describes the development of a system for CO_2 and CH_4 measurements on board the FAAM BAe-146 UK (Facility for Airborne Atmospheric Measurements, British Aerospace-146) atmospheric research aircraft using the cavity-enhanced absorption spectroscopy technique (CEAS). This system has been used during a number of recent airborne field projects. These include: the BORTAS campaign (quantifying the impact of BOReal forest fires on Tropospheric oxidants over the Atlantic using Aircraft and Satellites; Palmer et al., 2013), where the system was used to sample both fresh and aged plumes from Canadian boreal-biomass burning; the MAMM campaign (Methane and other greenhouse gases in the Arctic – Measurements, process studies and Modelling, http://www.arctic.ac.uk/mamm/), which is examining CH_4 sources at high northern latitudes; the SAMBBA campaign (South AMerican Biomass Burning Analysis, http://www.cas.manchester.ac.uk/resprojects/sambba/) ; and finally the system has been used to determine the natural gas leak rate from the Total Elgin gas platform in the North Sea (DECC, 2012). Firstly (Sect. 2), we describe the measurement set-up, optimisation, laboratory testing, in-flight calibration methodologies, data processing and quality control. In Sect. 3 the performance of the system is assessed through analysis of the in-flight calibrations and also by comparing to flask samples that were analysed for CO_2 and CH_4. Section 4 presents some of the first results from the system, where we calculate emission factors for Brazilian-biomass burning. A brief summary of the work is given in Sect. 5.

2 Experimental set-up

2.1 The CO_2, CH_4 and H_2O sensor

The infrared spectral region is widely used for spectroscopic detection of common atmospheric trace gases as many have strong absorption features within this region. One of the main challenges with direct laser absorption spectroscopy is to accurately measure small changes in laser intensity due to molecular absorption against a large, unabsorbed, background signal. Improvements in sensitivity can be made by increasing the path length through the sample so that a larger proportion of light is absorbed, e.g. by using multi-pass cells (McManus et al., 1995, 2010). In this study, CO_2, CH_4 and H_2O mole fraction measurements were made using a Fast Greenhouse Gas Analyser (FGGA, Model RMT-200), a commercially available instrument, from Los Gatos Research Ltd., USA, which we have subsequently modified to improve its performance for operation on board the UK FAAM BAe-146 research aircraft. This instrument uses a technique known either as cavity-enhanced absorption spectroscopy (CEAS) or off axis-integrated cavity output spectroscopy (OA-ICOS). This involves using an optical cavity to achieve an effective path length of several kilometres (Baer et al., 2002), which is many times longer than similar sized multi-pass cells (e.g. Herriot cells). The technique has been described in detail by Paul et al. (2001) and Baer et al. (2002). Briefly, a laser beam is aligned so that it enters an optical cavity at an angle to the cell optical axis. A steady state will be reached where the light intensity entering the cavity through one mirror is equal to the total of that either absorbed by

a molecular species or transmitted through the mirrors. The change in cavity output (ΔI) observed through one mirror due to a molecular species can then be related to the unabsorbed light intensity (I_0) by

$$\frac{\Delta I}{I_0} = \frac{G\,A}{1 + G\,A} \quad (1)$$

where, $G = R/(1-R)$, R is the mirror reflectivity, and A is the absorption due to a single pass of the cavity. A is given by $A = 1 - \exp(-\alpha(\upsilon, P, T)L\,C)$, where L is the distance between the mirrors, C is the concentration of the absorbing species and $\alpha(\upsilon, P, T)$ is its absorption cross section, which is a function of the frequency of the light, and the pressure and temperature of the cavity.

The FGGA uses two near infrared distributed feedback diode lasers, one to probe a CO_2 absorption line near 1.603 µm and the other to probe CH_4 and H_2O absorption lines near 1.651 µm. The laser frequency is rapidly scanned across the absorption features of interest by varying the laser injection current. Sample air is continuously pumped through the instrument detector cell, which comprises a 0.4 L optical cavity consisting of two high-reflectivity mirrors (reflectivity, $R > 0.9999$). Their reflectivity is continuously monitored by setting the laser to a non-absorbing wavelength at the end of each frequency sweep, then turning the laser off and measuring the cavity ring-down time, τ. τ is related to the mirror's reflectivity according to $R = [1 - L/(c\tau)]$, where c is the speed of light. A Voigt profile is subsequently fitted by least-squares regression to the transmitted spectrum and, using previously determined line strengths and positions from the HITRAN (high-resolution transmission) database (Rothman et al., 2009), together with the measured cavity temperature and pressure, the mole fraction of the absorbing species can be determined. The acquisition rate can be up to 10 Hz, but for this work the system was optimised for operation at 1 Hz.

This instrument and its predecessor model, the Fast Methane Analyser (FMA), previously have been successfully used for ground-based mole fraction and eddy covariance flux measurements (Hendriks et al., 2008; Tuzson et al., 2010). However, great care must be taken if the instrument is to be used on an aircraft due to the range and rapidly varying conditions that it will be subjected to, which can significantly alter its precision and stability. The object of this work was to develop a system capable of delivering precision and stability as close to laboratory operation as possible, which inevitably required more thorough and frequent calibration, optimisation of flow systems, sample lag times and attention to vibration and stability issues than ground based operation usually requires.

2.2 Flow-system assessment and improvements

To successfully install this and similar sensors on an aircraft, it is important to maintain the sample cavity pressure at a constant value over the range of inlet pressures that will be experienced during flight (in this case from ∼1000 to ∼250 mb). This is made more challenging due to the varying pressure fluctuations and vibrations that are encountered in-flight and potentially transmitted to the cavity. At higher cavity pressures, absorption increases resulting in a higher signal to noise ratio. However, it becomes harder to distinguish between individual line features due to pressure broadening from a reduced molecular mean free path. A set-point cavity pressure of 50 Torr was chosen, as a compromise between increased absorption and line-feature selectivity.

Figure 1 shows a schematic of both the instrument's sample-flow system and the calibration-gas system used. In situ measurements showed that the external diaphragm vacuum pump (N920APDCB, KNF Neuberger, UK) and electronic pressure controller (VSO-EP pressure control module, Parker Hannifin Corp, USA) used were able to maintain the instrument's cavity pressure at 50 Torr and a mass flow rate of ∼0.75 SLPM (standard liters per minute) over an altitude range of 0 to 9150 m with the throttle valve closed. The measured standard deviation of the cavity pressure across all flights was found to be only 0.07 Torr. However, above 9150 m the throttle valve had to be manually opened to maintain the cell pressure and the precision of the pressure control was slightly reduced.

Another major consideration when designing the aircraft's system inlet was to optimise the sample lines and flow components so as to achieve the shortest possible response time to external-gas mole fraction changes. High-spatial-resolution measurements are needed for many airborne applications where sharp, near source plumes have to be identified. This is particularly important as the system's real-time measurements may also be used to trigger the collection of whole-air samples while penetrating plumes of limited spatial extent.

The FGGA's aircraft inlet is mounted on a customised FAAM BAe-146 window blank (Avalon Aero Ltd, UK). Outboard and inboard views of the FAAM core chemistry instrumentation inlet window are shown in Fig. 2. The upper rearward facing 3/8″ (9.53 mm) OD (outer diameter) stainless-steel tube inlet (lined with 1/4″ (6.35 mm) OD PFA (perfluoroalkoxy) Teflon tube) is used for sampling CO and O_3. The lower rearward facing 3/8″ OD stainless-steel tube inlet is the dedicated FGGA inlet. While, the short 1/4″ OD rearward facing stainless-steel tube (in centre) is the calibrant outboard vent.

The inlet window is located adjacent to the core chemistry instrumentation rack, in place of starboard side window #14, to optimise the FGGA's sample-flow conductance and reduced lag times. Window #14 is located ∼14 m aft of the nose of the aircraft. At this distance, the 99 % thickness curve of the aircraft boundary layer, derived from computational fluid dynamics and the Engineering Sciences Data Unit (ESDU) item 79020 (BAe Systems, 2003) is ∼17 cm. The inlet tube was designed with an extra safety margin, so that

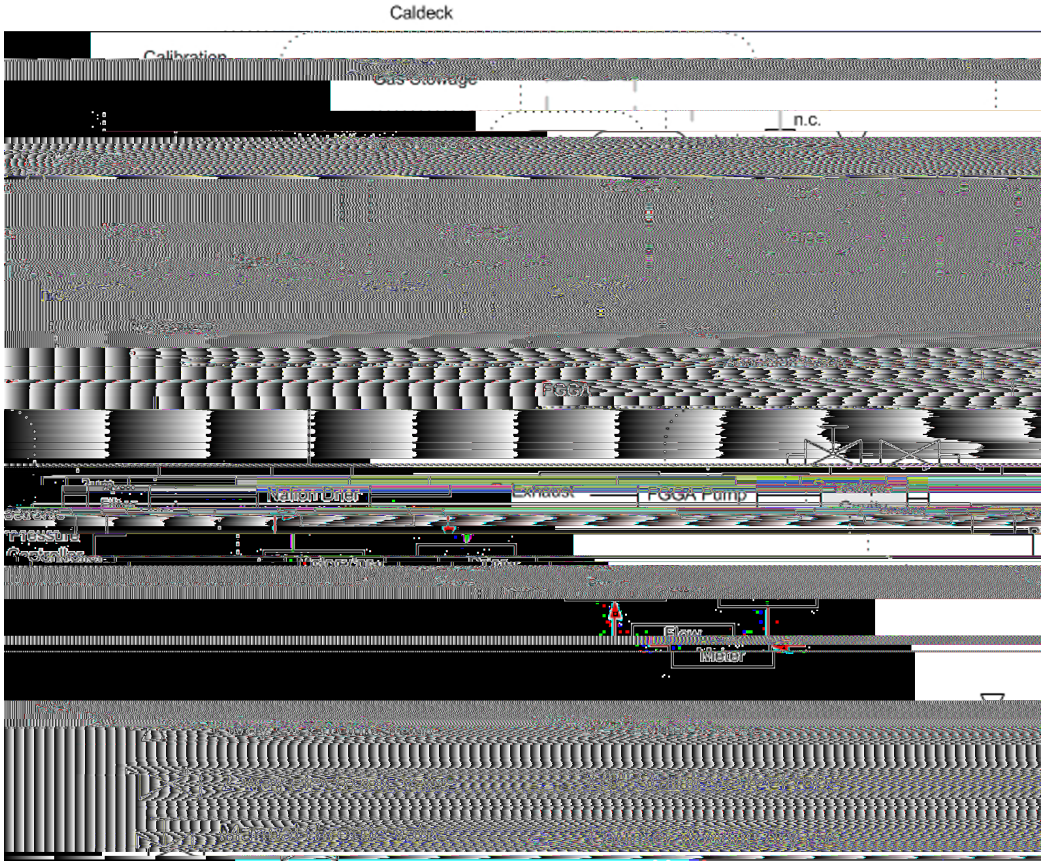

Fig. 1. A diagram of the sample and calibration air flow through the CO_2 and CH_4 system.

its tip protrudes ∼ 20 cm from the aircraft's skin, to guarantee free-flow sampling. This is an important factor considering the very high CO_2 concentrations present in the aircraft's pressurised cabin (> 700 ppm), which may leak into the external skin boundary layer, for instance via door seals, and thereby contaminate ambient air CO_2 measurements. Various test flights of this inlet configuration confirm that the inlet tip is standing in the free flow, with no discernible CO_2 contamination reported during roll, pitch and yaw-test manoeuvres.

The FGGA's instrument inlet is connected to the aircraft inlet using non-porous 1/4″ OD Eaton Synflex 1300 tubing, a material commonly used for sampling greenhouse gases. The total response time of the system is a combination of the time taken to travel through transfer lines from the aircraft inlet to the sample cavity plus the time taken for the instrument to respond fully to the change in mole fraction. Each of these were measured and assessed. First the inlet's lag time was determined by overflowing the inlet with N_2 and measuring the time taken to detect a change in mole fraction. The e-fold response time of the instrument cavity was determined by overflowing N_2 directly at the inlet bulkhead of the FGGA then computing an exponential fit to the observed signal decay. To simulate high-altitude sampling the tests were repeated at reduced inlet pressure by connecting a needle valve and a pressure sensor to the inlet. At 1007 mb inlet pressure the inlet lag time was 4.0 ± 1.0 s and the cavity's e-folding time was 1.4 ± 0.1 s. The response time was found to improve marginally with altitude, e.g. at 287 mb inlet pressure the inlet lag time was 2.0 ± 1.0 s and the e-folding time was 1.5 ± 0.1 s. This compares to the theoretical inlet lag times calculated using flow rates and pipe lengths (assuming plug-flow) of approximately ∼ 4.6 s at 1007 mb and ∼ 1.3 s at 287 mb.

During the system's first measurement campaign (BORTAS) a Nafion dryer was used to dry the sample before delivery to the instrument for analysis. This consisted of a multi-stranded exchange membrane (PD-50T-24MPS, Perma Pure Inc, USA) and a counter flowing dry gas stream created using a molecular sieve (81005, Alltech Associates Applied Science Ltd, UK) and a pump (G24/045, Gardner Denver Alton Ltd, UK). The reason for using this was to reduce the influence of rapidly changing H_2O on the retrieved mole fractions, which are described in Sect. 2.4. We found that the Nafion dryer was able to reduce the H_2O content of the sampled air to a small extent. However, during periods of sustained high-ambient humidity (e.g. when sampling in the marine boundary layer) H_2O exchange would occur in the opposite direction to that intended and the sample humidity

(a)

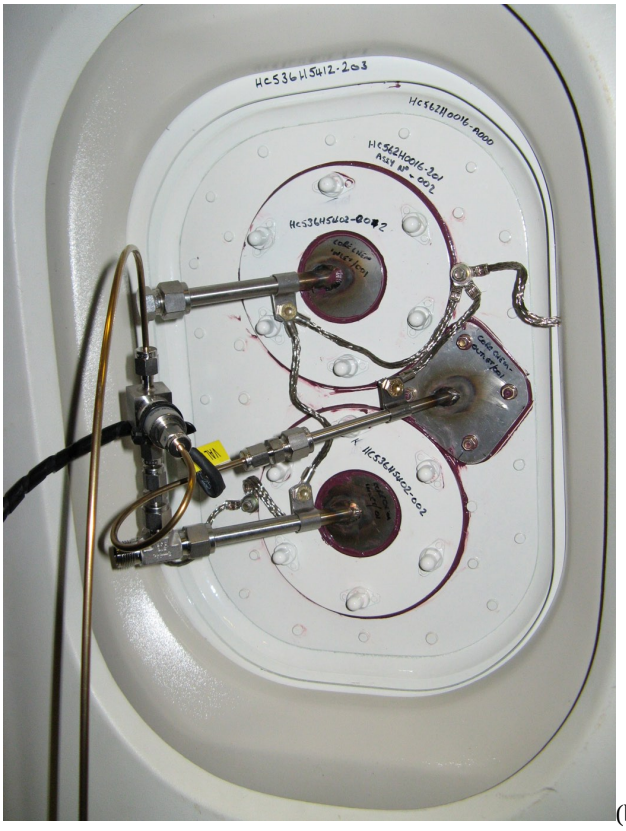

(b)

Fig. 2. (a) Outboard view of the FAAM core chemistry instrumentation inlet window fitted on starboard side window #14, under the FAAM BAe-146 wing. The lower 3/8″ OD rearward facing SS tube is the FGGA's dedicated inlet. The short 1/4″ OD rearward facing SS tube is the calibrant outboard vent. **(b)** Inboard view of FAAM core chemistry instrumentation inlet window. The 3-way calibration valve V1 is showed on the lower 3/8″ OD SS tube. The central 1/4″ OD tube is the calibrant outboard vent (connected to valve V1 normally open port).

would increase. This occurred to such a degree that there was little change in H_2O mole fraction between calibration and ambient sampling. The Nafion dryer was therefore removed from the system after the BORTAS campaign, with a view to improve inlet-flow conductance.

2.3 Gas standards and calibration system

CEAS and similar spectroscopic techniques are claimed as an absolute measurement approach, allowing mole fractions to be determined for specific gas molecules without the need for calibration. However, in practice, the terms in Eq. (1) can either not be measured or are not known with sufficient accuracy to achieve the desired high level of accuracy in the retrieved mole fractions. Thus routine in-flight calibrations are essential to identify and eliminate any drifts in the measurement system. Calibrations in this case were performed by regularly flushing the system with gas samples from one of three gas standard cylinders whose CO_2 and CH_4 mole fractions are given in Table 1. All three mixtures were traceable to the greenhouse-gas scales recommended by the WMO, a description of which is given for CH_4 by Dlugokencky et al. (2005) and for CO_2 by Zhao and Tans (2006).

The gas standards are held in 300 bar-rated, 10 L carbon-fibre hoop-wrap composite cylinders (BFC 124-136-002, Aluminium Alloy 7060, Luxfer, UK) and use Indutec series model C215 brass valves (Ceodeux Rotarex, Luxembourg) screwed into the cylinder collar with the aid of PTFE (polytetrafluoroethylene) thread tape. All three cylinders are horizontally mounted, to help reduce gravimetric fractionation (Keeling et al., 2007), in a separate custom-designed gas stowage (Mc Carthy Interiors Ltd., UK). The cylinders' brass regulators (part number 44-2212-244-1382, Tescom, UK) are used to pressurise, at 2.7 bar, three 1/8″ OD stainless-steel lines (part number 21512, Thames-Restek, UK) that bring the calibrants to the instrumentation rack on which the Caldeck and FGGA are mounted (see Fig. 1). Two 3-way valves and a 2-way valve (Series 9, 24Vdc solenoid valves, Parker Hannifin Corp, USA) are used to select when to flow the calibrant and from which cylinder. A mass flow controller (MCS-5SLPM, Alicat Scientific Inc, USA) is used to set the flow rate (up to 5 slpm) that either goes to vent (outboard) or to join the sample line, dependent on 3-way valve V1 in Fig. 1. This procedure allowed ambient measurements to continue to be made while the lines were being flushed before a calibration and the FGGA to stabilise on the calibration gas mole fraction more quickly. So that the calibrations mimicked ambient sampling conditions as closely as possible, the calibrant was arranged to join the sample line at the inlet on the window blank, allowing it to pass through the same path as ambient air (as shown in Fig. 1). This allowed the calibrant to create an overflow at the inlet preventing the sampling of ambient air. We found that using an overflow rather than a valve was a better method to switch between ambient air sampling and calibration gas, since it avoided sudden changes in

Table 1. The in-flight gas standards certified mole fractions used during the BORTAS and MAMM projects. The Max-Planck Institute for Biogeochemistry (Jena) carried out the calibration through the Infrastructure for Measurements of the European Carbon Cycle (EU 13 IMECC) project. A 6 month-mixture stability check showed the standards were stable over this period. The $\delta^{13}C$ isotopic ratios, determined using continuous-flow gas chromatography/isotope-ratio mass spectrometry (Fisher et al., 2006), are close enough to the ambient isotopic ratio so as not to cause a significant error in the measured mole fractions.

	CO_2 (ppm) $\pm 1\sigma$ EU 13 IMECC	CO_2 (ppm) $\pm 1\sigma$ 6 month stability check	$\delta^{13}C - CO_2$ ($^0/_{00}$) $\pm 1\sigma$ (count)	CH_4 (ppb) $\pm$ 1σ EU 13 IMECC	CH_4 (ppb) $\pm 1\sigma$ 6 month stability check	$\delta^{13}C - CH_4$ ($^0/_{00}$) $\pm 1\sigma$ (count)
High	489.27 ± 0.1	489.11 ± 0.04	-13.85 ± 0.03 (4)	2347.0 ± 1	2347.9 ± 0.2	-45.99 ± 0.03 (3)
Low	348.93 ± 0.04	349.10 ± 0.03	-9.89 ± 0.03 (3)	1891.1 ± 0.3	1891.2 ± 0.2	-47.12 ± 0.04 (3)
Target	388.38 ± 0.06	388.42 ± 0.03	-9.47 ± 0.03 (4)	1892.1 ± 0.8	1892.3 ± 0.2	-47.20 ± 0.06 (4)

the instrument's cavity pressure. The plumbing of calibration valve V1 immediately inboard on the inlet line employed a low dead-volume T-piece compression fitting, thereby minimising unswept volumes and unwanted mole fraction tailing following calibration. Figure 3 provides a time series of 1 Hz CO_2 data during a high/low span in-flight calibration, and illustrates the time response of the FGGA to the calibrant gas using the inlet configuration described above.

The three calibration cylinders, referred to as high, low and target, were filled to 300 bar at the University of East Anglia's Carbon Related Atmospheric Measurement (UEA-CRAM) Laboratory, using compressed air from outside the building that had been dried to a dew point of less than $-60\,°C$. The high was then made by adding a "spiking" mixture to the cylinder (CO_2 from an industrial source and CH_4 from a natural gas source), while the low was created using a series of chemical traps (Wilson et al., 2009). Unfortunately, the low CH_4 mole fraction could not be achieved at a sub-ambient level due to technical limitations with the UEA-CRAM CH_4 scrubbing stage in June 2011 (A. C. Manning, personal communication, 2011). The Max-Planck Institute for Biogeochemistry (Jena) carried out calibration of the gas standards as part of the Infrastructure for Measurements of the European Carbon Cycle project (EU 13 IMECC; see http://imecc.ipsl.jussieu.fr/).

Due to their large volume and high pressure the calibration cylinders could, in theory, last for over a year before they need to be refilled. However, gravimetric fractionation and pressure-dependent adsorption or desorption from the cylinder walls has previously been shown to limit the length of time that calibration gases can be stored (Langenfelds et al., 2005). CO_2 increases of up to 0.5 ppm have been observed at cylinder pressures below 30 bar. This is thought to be due to desorption from the cylinder walls that had previously been adsorbed at higher pressures (Daube et al., 2002; Chen et al., 2012). To safeguard against this we do not use the cylinders when the measured pressure drops below 35 bar. Permeation through some of the materials used in a cylinder's regulator has also been observed (Sturm et al., 2004; Chen et al., 2012).

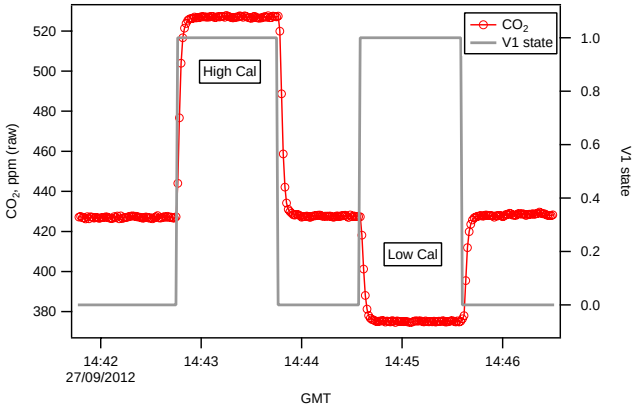

Fig. 3. In-flight high/low span calibration sequence performed during mission B742. The data shown are 1 Hz raw CO_2 ppm, acquired with the Los Gatos Research FGGA software.

There was very little information available in the literature on the stability of the gas cylinders, valves and regulators that we have used here, so to test how susceptible the in-flight standards were to the aforementioned effects they were re-analysed 6 months after filling, by the Greenhouse Gas Laboratory at Royal Holloway, University of London, using a cavity ring-down spectrometer (Model G2301, Picarro Inc, USA, calibrated to the EU 13 IMECC scale). The results of the re-analysis are given in Table 1. Within the analytical uncertainty, no change was found in the target CO_2 and the CH_4 mole fraction for all three mixtures. A change was observed in CO_2 for the low and high gas mixtures, which were 0.17 ppm lower and 0.16 ppm higher when re-analysed, respectively.

If the $^{13}C/^{12}C$ isotope ratio, for either CO_2 or CH_4, of the ambient air is significantly different to that of the calibration gases this can result in an incorrect measurement of the total CH_4 or CO_2. This is because the FGGA is only sensitive to $^{12}C^{16}O_2$ and $^{12}CH_4$ absorption lines. Therefore, when the system is calibrated, the measured $^{12}C^{16}O_2$ and $^{12}CH_4$ in the calibration cylinder is scaled to equal the total CO_2 and CH_4

from when the mixture was certified. The same scaling factor is applied to the ambient measurement to give the total CO_2 and CH_4 mole fraction. Since the calibration gases are not a completely natural mixture, they may have a significantly different isotopic composition to the sampled ambient air, the scaling factor used to determine the total CO_2 and CH_4 may no longer be valid.

For this reason, the ratio of the ^{13}C and ^{12}C isotopes of CO_2 and CH_4 in the calibration cylinders were determined, by Royal Holloway University's Greenhouse Gas Laboratory, using gas chromatography-continuous flow-isotope ratio mass spectrometry (GC-CF-IRMS) (Fisher et al., 2006). The results are also given in Table 1 and are expressed using δ notation on the VPDB scale (Vienna Pee Dee Belemnite). This isotopic effect has been estimated using 2 suites of NOAA standards at RHUL (Royal Holloway, University of London), one set of 3 with typical ambient-air isotopic signatures, and one set of 3 with synthetic air, with both CO_2 and CH_4 derived from natural gas.

Background $\delta^{13}C$-CO_2 is currently close to -8 ‰ (Allison and Francey, 2007) but is depleted by emissions of CO_2 from fossil fuel and combustion sources. While $\delta^{13}C$-CH_4 is typically -47.3 ‰ (Levin et al., 2012). For both species the high-span's $\delta^{13}C$ is furthest from these values and therefore will be responsible for the largest error. This could have been expected since the high-span gas mixture has been created with the largest proportion of the "spiking" mixture that was unlikely to have typical background isotopic ratios. If a sample is measured with typical background $\delta^{13}C$ and the same mole fraction as the high span the FGGA will overestimate its mole fraction by 0.03 ppm for CO_2 and 0.03 ppb for CH_4. For all the calibration mixtures the $\delta^{13}C$ values are similar enough to typical background values that the error from only measuring ^{12}C isotopologues, using the CEAS technique, is within the noise of the instrument. However, if plumes are measured that are significantly enriched in ^{13}C such as from biomass burning this will result in an underestimation of the total mole fraction (0.5 ppb at $\delta^{13}C - CH_4 = -27$ ‰). Other CO_2 and CH_4 isotopologues are less abundant and are thought to have a smaller effect (Tohjima et al., 2009; Chen et al., 2010).

2.4 Influence of water vapour

The variability of water vapour in the atmosphere, which covers several orders of magnitude and can be many percent in the troposphere, is large enough to cause significant deviations to the mole fractions retrieved using spectroscopy. This is due to three distinct mechanisms. Firstly, H_2O will cause a variable dilution of the CO_2 and CH_4 mole fraction. H_2O is the only species whose variability is large enough to cause changes to the CO_2 and CH_4 mole fraction of over about 0.1 %, purely due to a variable dilution throughout the troposphere. Secondly, H_2O has strong absorption lines in the infrared. Spectral interference due to H_2O either overlapping or near to the CO_2 or CH_4 absorption features of interest would likely alter the retrieved mole fractions. Finally, pressure broadening between the H_2O molecules and the analyte will alter the absorption-line shape. This is true of all molecules but the degree at which it occurs is dependent on the molecules involved and also the particular absorption line.

For these reasons, dry-air mole fractions, the number of moles of CO_2/CH_4 per the number of moles of dry air, need to be used if comparisons are to be made between different techniques, locations and with chemical transport models. These could be determined by drying the air sample before it is analysed. Previously, this approach has been employed successfully for airborne measurements of CO_2 and CH_4 using a combination of a Nafion dryers and dry-ice traps (Vay et al., 1999; Daube et al., 2002; Peischl et al., 2010). However, we have found that even when using the Nafion dryer, measured water vapour levels in the air sample were not sufficiently low to remove the aforementioned effects. Adding more dryers to the system would likely add complexity and weight, as well as further impact the instrument's time response, and at the same time increase the level of system maintenance needed. Therefore, we have opted to use the FGGA's simultaneous H_2O measurement to convert wet- to dry-air mole fractions.

Previously, the FGGA's on-board control computer software automatically removed the effects of dilution on the CO_2 or CH_4 mole fractions derived from the spectral fits, $[X]_{\mathrm{Wet}}$, using Eq. (2):

$$[X]_{\mathrm{Dilution}} = \frac{[X]_{\mathrm{Wet}}}{1 - 0.01\,[\mathrm{H_2O}]}, \quad (2)$$

where $[H_2O]$, % (cmol (mol)$^{-1}$), is the simultaneous measurement of H_2O in the instrument cavity. For this to work successfully, absolute accuracy of H_2O measurements are required. Based on this approach, in order to obtain the WMO recommended specification for CH_4 and CO_2 measurements, the corresponding H_2O measurement must have an absolute accuracy of 0.1 %.

To derive a theoretical correction for the effects of pressure broadening and spectral interference due to H_2O on the CO_2 and CH_4 measurements is more difficult, since the HITRAN database typically only contains information on the pressure-broadened line width within dry air (Brown et al., 2003). Here we use laboratory experiments to determine a relationship between the CO_2 and CH_4 wet-air mole fractions retrieved from the spectral fits and the corresponding dry-air mole fraction, incorporating all three effects into a single relationship. This approach is similar to previous work using other infrared absorption techniques (Neftel et al., 2010; Chen et al., 2010; Tuzson et al., 2010).

A schematic of the experimental set-up used is shown in Fig. 4. Air from a cylinder (12-N compressed air, BOC, UK), with nominal CO_2 and CH_4 mole fractions of 400 ppm and 2000 ppb, respectively, was passed through a dew-point

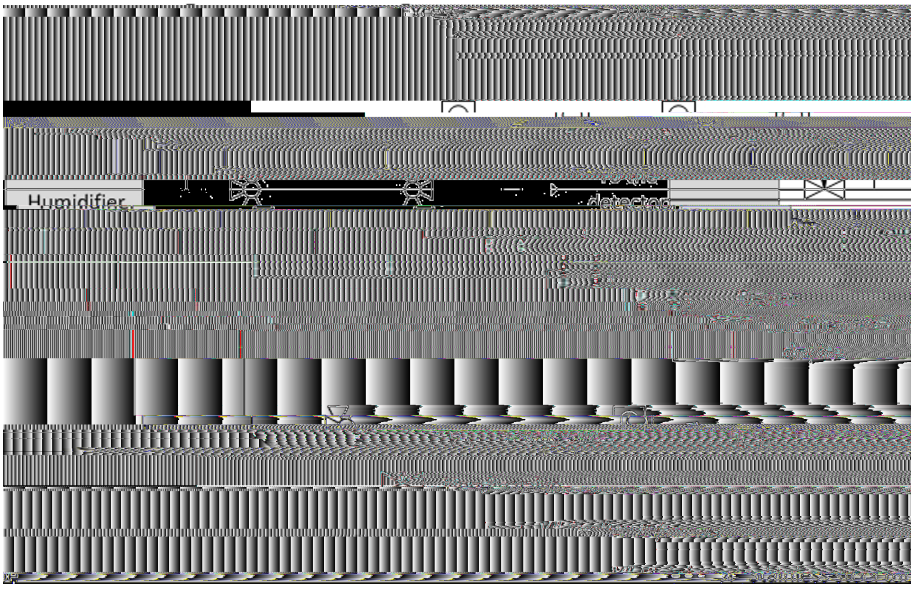

Fig. 4. A schematic of the experimental set-up used to determine how water vapour influences CO_2 and CH_4 measurements. The humidifier used was a Li-610 dew-point generator (Li-610, Li-Cor Inc., USA).

generator (Li-610, Li-Cor Inc., USA) creating a gas mixture that had a constant dry-air mole fraction of CO_2 and CH_4 but with a variable humidity controlled by the dew-point generator. Depending on the position of two 3-way valves, the gas mixture can be sent either directly to the FGGA or first through a stainless-steel coil that was within a dewar of dry ice. This lowers the dew point of the sample to less than −60 °C (0.002 %), which we approximate to be a measurement of the dry-air mole fraction of the cylinder.

The dew point was varied in 5 °C increments from 0 to 25 °C and back to 0 °C, which corresponds to the mole fractions 0.6 and 3.2 %, respectively. Between each change in the dew point, the two 3-way valves were switched to allow the FGGA to measure the air that had passed through the dry-ice trap. Once the system had stabilised, the signals from each period measuring dry air were averaged, interpolated and used to remove any drift in the CO_2 and CH_4 measurements. Throughout the experiment, the FGGA's water vapour measurement was consistently below that reported by the dew-point generator. A linear fit to the mole fraction from the dew-point generator versus the FGGA's measurement yielded an R^2 of 0.996, a regression slope of 1.526 ± 0.001 and an intercept of -0.65 ± 0.01 %. Since the dew-point generator had not been calibrated directly before these experiments, we do not consider it to be an absolute measurement, only a means to deliver variable humidity levels to the FGGA. Also, though the experiments were conducted in a temperature-controlled laboratory (temperature maintained at 28 °C), it is still possible that H_2O could condense on the walls of the tubing or the inlet filter. As a result, it is possible that the H_2O content that leaves the generator may not be identical to that which arrives at the sample cavity (LI-COR, 2004). When sampling the dry-gas stream the FGGA records a mean H_2O content of 0.013 % ($1\sigma = 0.008$ %).

This experiment was repeated three times over a three-month period, to test the repeatability of the system's response to varying humidity. The results are shown in Fig. 5 and suggest that using Eq. (2) alone to determine the dry-air mole fraction accurately is not sufficient. There was a clear relationship between the humidity and the simultaneous measurement of CO_2 and CH_4 even after Eq. (2) had been applied (Fig. 5, dashed lines). Instead we approximate the relationship between $[X]_{\mathrm{Wet}}$ and the corresponding dry-air mole fraction, $[X]_{\mathrm{Dry}}$, using a quadratic function of the form:

$$[X]_{\mathrm{Dry}} = \frac{[X]_{\mathrm{Wet}}}{a + b\,[\mathrm{H_2O}] + c\,[\mathrm{H_2O}]^2} \quad (3)$$

where a, b and c are the coefficients of the quadratic fit to $[X]_{\mathrm{Wet}}/[X]_{\mathrm{Dry}}$ versus $[H_2O]$, shown in Fig. 5. The determined fit coefficients are given in Table 2. To convert the fit residuals to mole fractions they have been multiplied by the nominal values 2000 ppb and 400 ppm. On the majority of occasions, the CH_4 residuals were typically less than 1 ppb, but there are two outliers at 2.9 and −2.11 ppb. For CO_2 they are generally less than 0.2 ppm. The standard deviations of all the residuals are 1.0 ppb and 0.15 ppm for CH_4 and CO_2, respectively. For this function to work successfully, absolute accuracy of H_2O measurements is not needed since any offset or non-unity response to varying H_2O should be accounted for in a, b and c. However, if the function is to be used over an extended period of time it is important that the H_2O measurement remains stable. There does not appear to

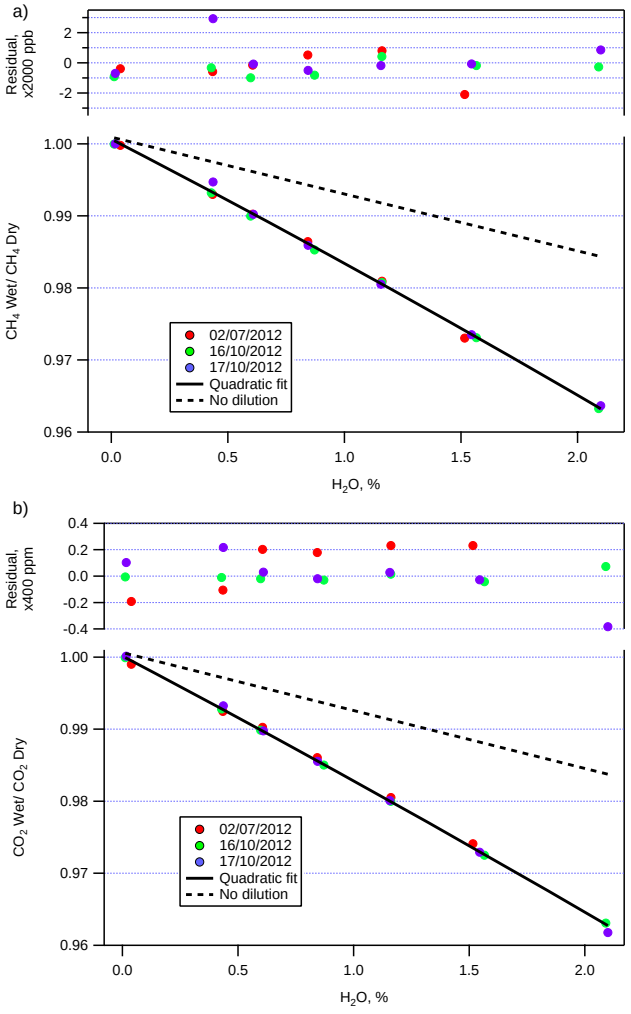

Fig. 5. The FGGA's response to varying humidity was determined by humidifying air from a cylinder. The dry measurements were determined by passing the humidified air through a dry-ice trap before it was analysed. This test was repeated three times over a three-month period to test the repeatability of the system. A relationship between the dry-air mole fraction and the measured wet-air mole fraction was determined using a quadratic fit to **(a)** CH_4 wet/CH_4 dry versus H_2O and **(b)** CO_2 wet/CO_2 dry versus H_2O. The dashed lines have been determined by applying Eq. (2) to CH_4 wet and CO_2 wet, this suggests that only correcting for the dilution effect due to H_2O is not sufficient to determine dry-air mole fractions.

be any distinction between when the tests were performed. Nevertheless, we do not yet feel that these experiments have been repeated over a long-enough timescale. So to further ensure the stability of the functions, these tests should and will be repeated before and after each future flying campaign.

2.5 Data processing and quality control

The high- and low-calibration mole fractions were chosen to span the range that would normally be encountered during flight. Measurements of these mixtures were used to rescale the dry-air mole fractions determined using Eq. (3) to the WMO scale. In-flight span calibrations were performed hourly. During a span calibration, gas from the high cylinder would first be flushed for 45 s through the system and then flowed through the FGGA's sample cavity for an additional 1 min. This procedure would be repeated for gas from the low cylinder, as shown in Fig. 3. The first 20 s of measurements were discarded to ensure the system had stabilised and the remaining 40 s of readings were averaged for both the high and low. A linear fit of the cylinder-calibration mole fraction versus the FGGA's measurement for sequential high and low calibrations was used to determine the FGGA's response slope and intercept values. These were linearly interpolated across the whole flight and applied to all ambient measurements placing the measurements on the WMO recommended scale.

Measurements of the target mixture were used to check the effectiveness of the rescaling and the instrument performance, the analysis of which is described in Sect. 3.1. Target calibrations were carried out several times between span calibrations under a variety of different flying conditions and altitudes.

As mentioned previously, it is important that the FGGA's cavity pressure is maintained at a constant value, chosen to be 50 Torr. Laboratory experiments running the system on air from a gas tank at different cavity pressures showed that deviations from this value caused a reduction in the instrument's precision (M. Gupta, personal communication, 2011). For this reason, if the recorded cavity pressure was ±5 % outside this set point, all the associated measurements were discarded.

Table 2. a, b and c are the coefficients of the quadratic fit to $[X]_{Wet}/[X]_{Dry}$ versus $[H_2O]$. These values can then be used to determine dry-air mole fractions using Eq. (3).

	a	b ($\%^{-1}$)	c ($\%^{-2}$)	Standard deviation of the fit residuals
CH_4	1.0006	−0.016697	−0.000533	1.0 ppb
CO_2	1.0001	−0.016889	−0.000444	0.15 ppm

3 Instrument characterisation

3.1 Accuracy and precision

To assess the short-term precision of the system we use the Allan variance technique (Werle et al., 1993). Whilst sampling a compressed-air cylinder in the laboratory, 1 Hz (1σ) precisions of 1.88 ppb for CH_4 and 0.41 ppm for CO_2 are typically obtained. The commercially available version of the

FGGA normally operates at 140 Torr cavity pressure, rather than the 50 Torr used in this work. However, as long as the fitting routines are updated for the specific cavity pressure (M. Gupta, personal communication, 2011), 1 Hz precisions are found to be broadly comparable between 50 and 140 Torr operation. This degree of precision can be replicated in-flight, for example 1 Hz precisions are found to be typically 1.61 ppb for CH_4 and 0.40 ppm for CO_2 . This suggests that as long as the instrument's cavity pressure is maintained with sufficient precision, the CEAS technique employed by the FGGA is well suited for airborne measurements.

The in-flight measurements of the target gas mixture are used to assess long-term repeatability and accuracy of the system's airborne measurements. Figure 6 shows the in-flight target measurements, once the data had been rescaled to the WMO scale, for all flights when the system was operated between 11 July 2011 and 3 May 2012. The data set comprised a total of 29 flights. There is only a small offset in the FGGA measurement compared to the target certification, the mean difference between the measurements and the certified-target mole fraction was −0.07 ppb for CH_4 and −0.06 ppm for CO_2. The frequency distribution of the target measurements for CO_2 was approximately Gaussian. However, the CH_4 measurements appeared to have a small drift in the system that was not captured by the span calibrations so the distribution of target calibrations do not show quite as good agreement with the assumed Gaussian fit as it does for CO_2. At 1 Hz the standard deviation of the frequency distribution is 2.48 ppb and 0.66 ppm for CH_4 and CO_2, respectively. If the measurements are averaged to 10 s this drops to 2.00 ppb and 0.45 ppm. Through the addition of all known uncertainties we estimate a total accuracy of ±1.28 ppb for CH_4 (H_2O correction 1σ fit residual ±1 ppb, target standard calibration ±0.8 ppb and in-flight target measurement ±0.07 ppb) and ±0.17 for CO_2 (H_2O correction 1σ fit residual ±0.15 ppm, target standard calibration ±0.06 ppm and in-flight target measurement ±0.06 ppm).

As mentioned previously, during the BORTAS flights the system was operated with a Nafion dryer. The performance of the system was found to be no worse when the dryer was used (11 July 2011–23 July 2011) compared to those flights when it was not (24 November 2011–3 May 2012). The lack of deviation between the measured target mixture and its calibration suggests that permeation of CO_2 and CH_4 through the membrane is small, which is in agreement with work by other groups (Vay et al., 1999).

3.2 Comparison between in situ and whole-air sample measurements

During two flights when the FGGA was operated (flight number B682 on 14 March 2012 and B685 on 18 March 2012), 26 whole-air samples were also collected in stainless-steel sample flasks. A description of the sample flasks can be found in Lewis et al. (2013). These

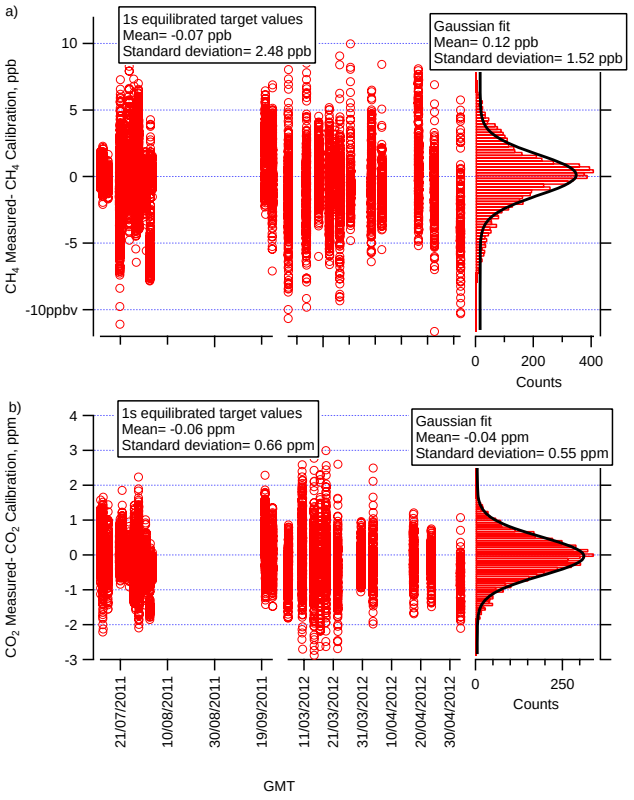

Fig. 6. An estimate of the system's accuracy can be made by examining the difference between the calibration mole fraction and the scaled FGGA measurement of the target gas mixture. At 1 Hz the mean ±1 standard deviation difference between the two is -0.07 ± 2.48 ppb for CH_4 and -0.06 ± 0.66 ppb for CO_2.

flasks were analysed post-flight for CO_2 and CH_4, by Royal Holloway University's Greenhouse Gas Laboratory, using CRDS, (Model G2301, Picarro Inc, USA, calibrated to the EU 13 IMECC scale), with a reported accuracy of 0.5 ppb and 0.1 ppm for CH_4 and CO_2, respectively. This provided a second method to validate the in-flight FGGA measurements. For a direct comparison the 1 Hz in situ data were averaged over the recorded filling times of the flasks, this was typically between 20 and 60 s. Figure 7 shows the scatter plot of the mole fraction derived from both techniques. The average deviation between the two methods (the FGGA measurement minus the flask measurement averaged for all 26 samples) was −2.4 ppb (1σ = 2.3 ppb) for CH_4 and −0.22 ppm (1σ = 0.45 ppm) for CO_2. For both species this is slightly larger than the estimate of the FGGA's accuracy from the in-flight calibrations.

Both the in situ and flask sample measurements were made using instruments calibrated to the same WMO scales. Since the only difference between calibration and ambient sampling should be that the calibration gases do not contain H_2O, the extra deviation could be attributed to one or both of the analysers not correctly computing dry-air mole fractions.

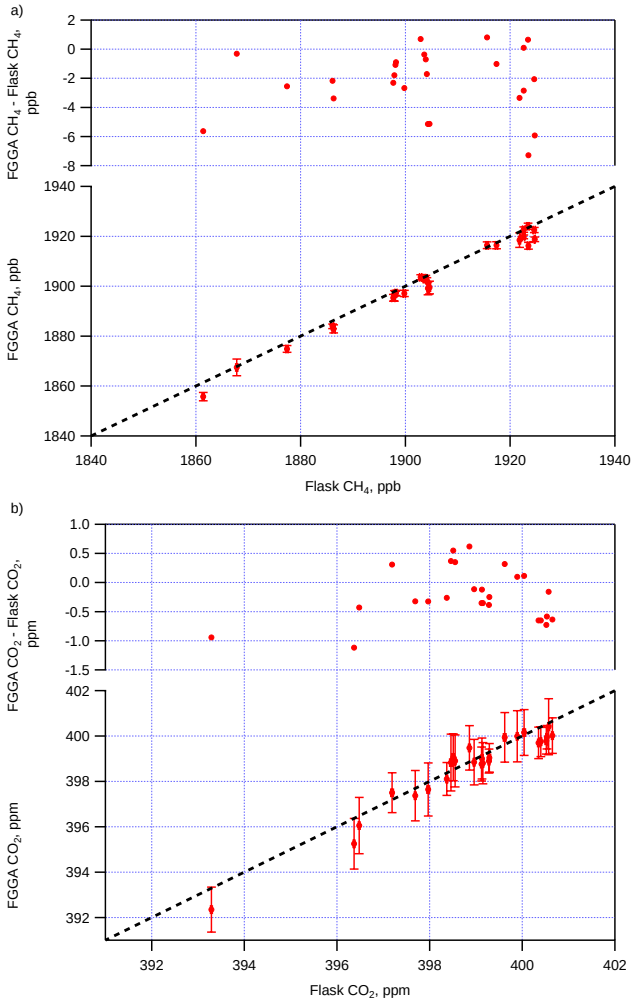

Fig. 7. Scatter plots of FGGA versus whole-air sample measurements of **(a)** CH_4 and **(b)** CO_2. Whole-air samples were collected in flasks and analysed post flight using CRDS (Model G2301, Picarro Inc, USA). The FGGA's original 1 Hz measurements were averaged over the filling period of each flask. Error bars are the standard deviation of the FGGA measurements during each filling period, indicating the uncertainty in the averaging of the in situ measurements. The dotted line is the one-to-one relationship.

However, a direct comparison between the two techniques is complicated as it is assumed that the flasks are filled at a constant rate and this is not thought to be the case, particularly at different altitudes. Therefore, a constant averaging window may not be appropriate. However, with this caveat, the standard deviation of the 1 Hz measurements has been included in Fig. 7, as error bars, to show the variability in CO_2 and CH_4 during the filling period and as a measure of the uncertainty during the sample period. Previous work has shown that agreement between in situ and whole-air sample measurements can improve if a weighting function is used; however, in order to derive this function, the pressure in the flask during the flushing and filling process needs to be known (Chen et al., 2012). Unfortunately, this information is not currently available on our aircraft and the comparison must therefore be subject to this caveat.

It is also conceivable that the content of the flask has been altered in the two-week period between filling and analysis, due to similar mechanisms to those described in Sect. 2.4. However, no variations of this magnitude have previously been detected.

4 Airborne measurements in biomass-burning plumes

The system's measurements, made as part of the BORTAS and MAMM projects, as well those assessing the Total Elgin gas-platform leak rate will be presented in separate papers. To highlight the instrument capability based on the above work we show example data, when the system was used to sample biomass-burning plumes, as part of the SAMBBA campaign. During this experiment, measurement-flight number B742 was carried out on 27 September 2012. This consisted of flying in the boundary layer over an active fire region near Palmas, Brazil ($\sim 11.1°$ S, $\sim 47.3°$ W), a region containing a mixture of grassland and forests. During this flight a number of biomass-burning plumes were intercepted with both CO_2 and CH_4 mole fractions significantly enhanced above their local background levels. Sampling these near source plumes are some of the most challenging measurements that the system will be used for due to the limited time spent within the plumes and the large and rapid changes in mole fractions.

Figure 8 shows that the enhancements in CO_2 and CH_4 correspond well with coincident measurements of CO made on board the FAAM BAe-146. The CO measurements were determined using a VUV (vacuum ultraviolet) fast-fluorescence analyser, accurate to 2 % (AL5002, Aerolaser GmbH, Germany; Gerbig et al., 1999). The CO measurements were used to determine an emission ratio, a commonly used measure of emissions from biomass burning, representing the proportion of a species emitted by the fires relative to a tracer species. The emission ratio can be calculated as the regression slope of the in-plume measurements of the species of interest relative to a tracer species for biomass burning. Due to the excellent correlation with CO we do not distinguish between individual plumes. Instead we calculate emission ratios, relative to CO, for the whole of the low level portion of flight B742, we find these to be 14.77 ± 0.03 mol CO_2 (mol CO)$^{-1}$ and 0.0532 ± 0.0001 mol CH_4 (mol CO)$^{-1}$. This means that the emission ratios we calculate are the combination of several fires in a small region. By assuming a carbon content of the soils these emission ratios can be converted to emission factors, an estimate of the mass of the species emitted per unit mass of biomass burnt. We use the methodology detailed by Yokelson et al. (1999) to determine emission factors of 1710 ± 171 g (kg dry matter)$^{-1}$ for CO_2 and 2.2 ± 0.2 g

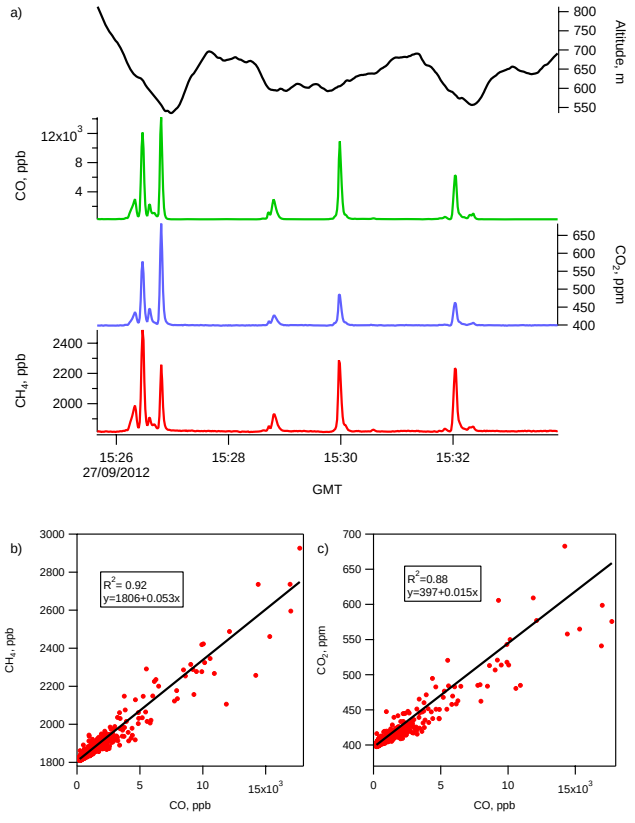

Fig. 8. (a) Shows a time series whilst flying in the boundary layer during flight B742 where a number of biomass-burning plumes were intercepted near Palmas, Brazil. Scatter plots for **(b)** CH_4 and **(c)** CO_2 both show strong correlation with CO and allow emission ratios to be determined, which were found to be 14.77 ± 0.03 mol CO_2 (mol CO)$^{-1}$ and 0.0532 ± 0.0001 mol CH_4 (mol CO)$^{-1}$.

(kg dry matter)$^{-1}$ for CH_4. These are in excellent agreement with values in the literature for savannah and grassland fires. Andreae and Merlet (2001) report average literature values of 1613 ± 95 g (kg dry matter)$^{-1}$ and 2.3 ± 0.9 g (kg dry matter)$^{-1}$ for CO_2 and CH_4, respectively for savannah and grassland fires.

5 Conclusions

A system for continuous airborne measurements of CO_2 and CH_4 has been developed for operation on board the FAAM BAe-146 UK research aircraft. The system is shown to be capable of sampling both boundary-layer plumes and the upper troposphere/lower stratosphere (UTLS), over an altitude range of 0 to 9153 m. Data from 29 sampling flights were used to assess the operational accuracy of the system. Analysis of the in-flight calibrations suggests that the long-term 1 Hz measurements from the system are accurate to 1.28 ppb (1σ repeatability at 1 Hz = 2.48 ppb) for CH_4 and 0.17 ppm (1σ repeatability at 1 Hz = 0.66 ppm) for CO_2 compared with WMO traceable standards. No motion or altitude dependant behaviour was detected in these calibrations. When the system was compared to whole-air samples there was a mean difference between the two techniques of -2.4 ppb ($1\sigma = 2.3$ ppb) for CH_4 and -0.22 ppm ($1\sigma = 0.45$ ppm) for CO_2.

The system did not incorporate a drying stage to remove H_2O in the sample to < 0.1 %. Therefore, it was necessary to use the simultaneous H_2O measurement to remove the effects of H_2O on the spectroscopic retrieval of CO_2 and CH_4. Previously, the FGGA only accounted for the dilution effect of H_2O to determine the dry-air mole fraction of a species. Laboratory experiments measuring air from a cylinder at different humidities suggest that this is not sufficient. From these experiments, new correction functions have been determined. These experiments were repeated three times over a three-month period and the errors with the correction functions were found to be 1.0 ppb and 0.15 ppm for CH_4 and CO_2, respectively. However, since this is only based on three experiments further repeats are planned for before and after every flying campaign in which the system is used. These corrections will be routinely provided for the future FAAM FGGA data sets.

The ability of the system to sample near source plumes of limited spatial extent was highlighted when it was used to calculate emission factors for biomass-burning plumes, in the savannah regions near Palmas, Brazil, as part of the SAMBBA experiment. The determined emission factors of 1710 ± 171 g (kg dry matter)$^{-1}$ for CO_2 and 2.2 ± 0.2 g (kg dry matter)$^{-1}$ for CH_4 are in excellent agreement with previous studies.

Future work on the system will involve improving the instrument's response time to allow airborne eddy covariance flux measurements. This will require the installation of a high-flow-displacement external pump (e.g. Edwards Vacuum XDS35i or nXDS20).

Acknowledgements. The authors wish to thank in particular T. Ryerson (NOAA), J. Peischl (NOAA), B. Stephens (NCAR), A. Manning (UEA, Norwich, UK), P. Wilson (UEA, Norwich, UK), J. Muller (Uni. Manchester, UK) and M. Gupta (Los Gatos Research, Ltd), for useful discussions about greenhouse gas measurements and calibration. We are grateful to S. Tooley and J. Smith (Avalon Aero Ltd, UK) for their help with the design and certification of the aircraft instrument rack. We would like to thank FAAM staff and all those involved with the SAMBBA project. S. J. O'Shea is in receipt of a NERC PhD studentship. Part of this work was supported by the NERC project, Methane and Other Greenhouse Gases in the Arctic – Measurements, Process Studies and Modelling (MAMM), grant #NE/I029161/1.

Edited by: M. von Hobe

References

Allison, C. E. and Francey, R. J.: Verifying Southern Hemisphere trends in atmospheric carbon dioxide stable isotopes, J. Geophys. Res.-Atmos., 112, D21304, doi:10.1029/2006jd007345, 2007.

Andreae, M. O. and Merlet, P.: Emission of trace gases and aerosols from biomass burning, Global Biogeochem. Cy., 15, 955–966, doi:10.1029/2000gb001382, 2001.

Aydin, M., Verhulst, K. R., Saltzman, E. S., Battle, M. O., Montzka, S. A., Blake, D. R., Tang, Q., and Prather, M. J.: Recent decreases in fossil-fuel emissions of ethane and methane derived from firn air, Nature, 476, 198–201, doi:10.1038/nature10352, 2011.

BAe Systems 146 Atmospheric Research Aircraft: Location of Inlets and Sensors In Relation to the Boundary Layer, document number ADE-46D-R-463-000792, BAE SYSTEMS, UK, 3 November 2003.

Baer, D. S., Paul, J. B., Gupta, J. B., and O'Keefe, A.: Sensitive absorption measurements in the near-infrared region using off-axis integrated-cavity-output spectroscopy, Appl. Phys. B, 75, 261–265, doi:10.1007/s00340-002-0971-z, 2002.

Baker, A. K., Schuck, T. J., Brenninkmeijer, C. A. M., Rauthe-Schoech, A., Slemr, F., van Velthoven, P. F. J., and Lelieveld, J.: Estimating the contribution of monsoon-related biogenic production to methane emissions from South Asia using CARIBIC observations, Geophys. Res. Lett., 39, L10813, doi:10.1029/2012gl051756, 2012.

Bousquet, P., Ringeval, B., Pison, I., Dlugokencky, E. J., Brunke, E.-G., Carouge, C., Chevallier, F., Fortems-Cheiney, A., Frankenberg, C., Hauglustaine, D. A., Krummel, P. B., Langenfelds, R. L., Ramonet, M., Schmidt, M., Steele, L. P., Szopa, S., Yver, C., Viovy, N., and Ciais, P.: Source attribution of the changes in atmospheric methane for 2006–2008, Atmos. Chem. Phys., 11, 3689–3700, doi:10.5194/acp-11-3689-2011, 2011.

Brown, L. R., Chris Benner, D., Champion, J. P., Devi, V. M., Fejard, L., Gamache, R. R., Gabard, T., Hilico, J. C., Lavorel, B., Loete, M., Mellau, G. C., Nikitin, A., Pine, A. S., Predoi-Cross, A., Rinsland, C. P., Robert, O., Sams, R. L., Smith, M. A. H., Tashkun, S. A., and Tyuterev, V. G.: Methane line parameters in HITRAN, J. Quant. Spectrosc. Ra., 82, 219–238, 2003.

Chen, H., Winderlich, J., Gerbig, C., Hoefer, A., Rella, C. W., Crosson, E. R., Van Pelt, A. D., Steinbach, J., Kolle, O., Beck, V., Daube, B. C., Gottlieb, E. W., Chow, V. Y., Santoni, G. W., and Wofsy, S. C.: High-accuracy continuous airborne measurements of greenhouse gases (CO_2 and CH_4) using the cavity ring-down spectroscopy (CRDS) technique, Atmos. Meas. Tech., 3, 375–386, doi:10.5194/amt-3-375-2010, 2010.

Chen, H., Winderlich, J., Gerbig, C., Katrynski, K., Jordan, A., and Heimann, M.: Validation of routine continuous airborne CO_2 observations near the Bialystok Tall Tower, Atmos. Meas. Tech., 5, 873–889, doi:10.5194/amt-5-873-2012, 2012.

Daube, B. C., Boering, K. A., Andrews, A. E., and Wofsy, S. C.: A high-precision fast-response airborne CO_2 analyzer for in situ sampling from the surface to the middle stratosphere, J. Atmos. Ocean. Tech., 19, 1532–1543, 2002.

DECC (UK Department for Energy and Climate Change): Elgin Gas Release, Government Interest Group update of environmental aspects relating to the incident, http://og.decc.gov.uk/media/viewfile.ashx?filetype=4&filepath=og/environment/5283-elgin-gas-release-gig-update1.doc&minwidth=true (last access: 22 November 2012), 11 April 2012.

Dentener, F., Peters, W., Krol, M., van Weele, M., Bergamaschi, P., and Lelieveld, J.: Interannual variability and trend of CH_4 lifetime as a measure for OH changes in the 1979-1993 time period, J. Geophys. Res.-Atmos., 108, 4442, doi:10.1029/2002jd002916, 2003.

Deutscher, N. M., Griffith, D. W. T., Bryant, G. W., Wennberg, P. O., Toon, G. C., Washenfelder, R. A., Keppel-Aleks, G., Wunch, D., Yavin, Y., Allen, N. T., Blavier, J.-F., Jiménez, R., Daube, B. C., Bright, A. V., Matross, D. M., Wofsy, S. C., and Park, S.: Total column CO_2 measurements at Darwin, Australia – site description and calibration against in situ aircraft profiles, Atmos. Meas. Tech., 3, 947–958, doi:10.5194/amt-3-947-2010, 2010.

Dlugokencky, E. J., Walter, B. P., Masarie, K. A., Lang, P. M., and Kasischke, E. S.: Measurements of an anomalous global methane increase during 1998, Geophys. Res. Lett., 28, 499–502, doi:10.1029/2000gl012119, 2001.

Dlugokencky, E. J., Myers, R. C., Lang, P. M., Masarie, K. A., Crotwell, A. M., Thoning, K. W., Hall, B. D., Elkins, J. W., and Steele, L. P.: Conversion of NOAA atmospheric dry air CH_4 mole fractions to a gravimetrically prepared standard scale, J. Geophys. Res.-Atmos., 110, D18306, doi:10.1029/2005jd006035, 2005.

Dlugokencky, E. J., Bruhwiler, L., White, J. W. C., Emmons, L. K., Novelli, P. C., Montzka, S. A., Masarie, K. A., Lang, P. M., Crotwell, A. M., Miller, J. B., and Gatti, L. V.: Observational constraints on recent increases in the atmospheric CH_4 burden, Geophys. Res. Lett., 36, L18803, doi:10.1029/2009gl039780, 2009.

Dlugokencky, E. J., Nisbet, E. G., Fisher, R., and Lowry, D.: Global atmospheric methane: budget, changes and dangers, Philos. T. Roy. Soc. A, 369, 2058–2072, doi:10.1098/rsta.2010.0341, 2011.

Etheridge, D. M., Steele, L. P., Francey, R. J., and Langenfelds, R. L.: Atmospheric methane between 1000 AD and present: Evidence of anthropogenic emissions and climatic variability, J. Geophys. Res.-Atmos., 103, 15979–15993, doi:10.1029/98jd00923, 1998.

Fiore, A. M., Horowitz, L. W., Dlugokencky, E. J., and West, J. J.: Impact of meteorology and emissions on methane trends, 1990–2004, Geophys. Res. Lett., 33, L12809, doi:10.1029/2006gl026199, 2006.

Fisher, R., Lowry, D., Wilkin, O., Sriskantharajah, S., and Nisbet, E. G.: High-precision, automated stable isotope analysis of atmospheric methane and carbon dioxide using continuous-flow isotope-ratio mass spectrometry, Rapid Commun. Mass Spectrom., 20, 200–208, doi:10.1002/rcm.2300, 2006.

Forster, P. and Ramaswamy, V.: Changes in Atmospheric Constituents and in Radiative Forcing, Climate Change 2007: the Physical Science Basis, Cambridge Univ. Press, Cambridge, UK, 129–234, 2007.

Gerbig, C., Schmitgen, S., Kley, D., Volz-Thomas, A., Dewey, K., and Haaks, D.: An improved fast-response vacuum-UV resonance fluorescence CO instrument, J. Geophys. Res.-Atmos., 104, 1699–1704, doi:10.1029/1998jd100031, 1999.

Hendriks, D. M. D., Dolman, A. J., van der Molen, M. K., and van Huissteden, J.: A compact and stable eddy covariance set-up for methane measurements using off-axis integrated cavity output spectroscopy, Atmos. Chem. Phys., 8, 431–443, doi:10.5194/acp-8-431-2008, 2008.

Kai, F. M., Tyler, S. C., Randerson, J. T., and Blake, D. R.: Reduced methane growth rate explained by decreased

Northern Hemisphere microbial sources, Nature, 476, 194–197, doi:10.1038/nature10259, 2011.

Keeling, C. D., Harris, T. B., and Wilkins, E. M.: Concentration of Atmospheric Carbon Dioxide at 500 and 700 Millibars, J. Geophys. Res., 73, 4511–4528, 1968.

Keeling, R. F., Manning, A. C., Paplawsky, W. J., and Cox, A. C.: On the long-term stability of reference gases for atmospheric O_2/N_2 and CO_2 measurements, Tellus B, 59, 3–14, doi:10.1111/j.1600-0889.2006.00228.x, 2007.

Kort, E. A., Patra, P. K., Ishijima, K., Daube, B. C., Jimenez, R., Elkins, J., Hurst, D., Moore, F. L., Sweeney, C., and Wofsy, S. C.: Tropospheric distribution and variability of N_2O: Evidence for strong tropical emissions, Geophys. Res. Lett., 38, L15806, doi:10.1029/2011gl047612, 2011.

Kort, E. A., Wofsy, S. C., Daube, B. C., Diao, M., Elkins, J. W., Gao, R. S., Hintsa, E. J., Hurst, D. F., Jimenez, R., Moore, F. L., Spackman, J. R., and Zondlo, M. A.: Atmospheric observations of Arctic Ocean methane emissions up to 82 degrees north, Nat. Geosci., 5, 318–321, doi:10.1038/ngeo1452, 2012.

Langenfelds, R. L., Francey, R. J., Pak, B. C., Steele, L. P., Lloyd, J., Trudinger, C. M., and Allison, C. E.: Interannual growth rate variations of atmospheric CO_2 and its $\delta^{13}C$, H_2, CH_4, and CO between 1992 and 1999 linked to biomass burning, Global Biogeochem. Cy., 16, 1048, doi:10.1029/2001gb001466, 2002.

Langenfelds, R. L., van der Schoot, M. V., Francey, R. J., Steele, L. P., Schmidt, M., and Mukai, H.: Modification of air standard composition by diffusive and surface processes, J. Geophys. Res.-Atmos., 110, D13307, doi:10.1029/2004jd005482, 2005.

Levin, I., Veidt, C., Vaughn, B. H., Brailsford, G., Bromley, T., Heinz, R., Lowe, D., Miller, J. B., Poss, C., and White, J. W. C.: No inter-hemispheric $\delta^{13}CH_4$ trend observed, Nature, 486, 194–197, doi:10.1038/nature11175, 2012.

Lewis, A. C., Evans, M. J., Hopkins, J. R., Punjabi, S., Read, K. A., Purvis, R. M., Andrews, S. J., Moller, S. J., Carpenter, L. J., Lee, J. D., Rickard, A. R., Palmer, P. I., and Parrington, M.: The influence of biomass burning on the global distribution of selected non-methane organic compounds, Atmos. Chem. Phys., 13, 851–867, doi:10.5194/acp-13-851-2013, 2013.

LI-COR: LI-610 Portable Dew Point Generator Instruction Manual v11, LI-COR, Inc, USA, 2004.

Lin, J. C., Gerbig, C., Wofsy, S. C., Daube, B. C., Matross, D. M., Chow, V. Y., Gottlieb, E., Andrews, A. E., Pathmathevan, M., and Munger, J. W.: What have we learned from intensive atmospheric sampling field programmes of CO_2?, Tellus B, 58, 331–343, doi:10.1111/j.1600-0889.2006.00202.x, 2006.

Marquis, M. and Tans, P.: Climate change – Carbon crucible, Science, 320, doi:10.1126/science.1156451, 2008.

McManus, J. B., Kebabian, P. L., and Zahniser, W. S.: Astigmatic mirror multi-pass absorption cell for long-path-length spectroscopy, Appl. Optics, 34, 3336–3348, 1995.

McManus, J. B., Zahniser, M. S., Nelson Jr., D. D., Shorter, J. H., Herndon, S., Wood, E., and Wehr, R.: Application of quantum cascade lasers to high-precision atmospheric trace gas measurements, Opt. Engin., 49, 111124, doi:10.1117/1.3498782, 2010.

Neftel, A., Ammann, C., Fischer, C., Spirig, C., Conen, F., Emmenegger, L., Tuzson, B., and Wahlen, S.: N_2O exchange over managed grassland: Application of a quantum cascade laser spectrometer for micrometeorological flux measurements, Agr. Forest Meteorol., 150, 775–785, doi:10.1016/j.agrformet.2009.07.013, 2010.

Palmer, P. I., Parrington, M., Lee, J. D., Lewis, A. C., Rickard, A. R., Bernath, P. F., Duck, T. J., Waugh, D. L., Tarasick, D. W., Andrews, S., Aruffo, E., Bailey, L. J., Barrett, E., Bauguitte, S. J.-B., Curry, K. R., Di Carlo, P., Chisholm, L., Dan, L., Forster, G., Franklin, J. E., Gibson, M. D., Griffin, D., Helmig, D., Hopkins, J. R., Hopper, J. T., Jenkin, M. E., Kindred, D., Kliever, J., Le Breton, M., Matthiesen, S., Maurice, M., Moller, S., Moore, D. P., Oram, D. E., O'Shea, S. J., Christopher Owen, R., Pagniello, C. M. L. S., Pawson, S., Percival, C. J., Pierce, J. R., Punjabi, S., Purvis, R. M., Remedios, J. J., Rotermund, K. M., Sakamoto, K. M., da Silva, A. M., Strawbridge, K. B., Strong, K., Taylor, J., Trigwell, R., Tereszchuk, K. A., Walker, K. A., Weaver, D., Whaley, C., and Young, J. C.: Quantifying the impact of BOReal forest fires on Tropospheric oxidants over the Atlantic using Aircraft and Satellites (BORTAS) experiment: design, execution and science overview, Atmos. Chem. Phys. Discuss., 13, 4127–4181, doi:10.5194/acpd-13-4127-2013, 2013.

Patra, P. K., Niwa, Y., Schuck, T. J., Brenninkmeijer, C. A. M., Machida, T., Matsueda, H., and Sawa, Y.: Carbon balance of South Asia constrained by passenger aircraft CO_2 measurements, Atmos. Chem. Phys., 11, 4163–4175, doi:10.5194/acp-11-4163-2011, 2011.

Paul, J. B., Lapson, L., and Anderson, J. G.: Ultrasensitive absorption spectroscopy with a high-finesse optical cavity and off-axis alignment, Appl. Optics, 40, 4904–4910, doi:10.1364/ao.40.004904, 2001.

Peischl, J., Ryerson, T. B., Holloway, J. S., Parrish, D. D., Trainer, M., Frost, G. J., Aikin, K. C., Brown, S. S., Dube, W. P., Stark, H., and Fehsenfeld, F. C.: A top-down analysis of emissions from selected Texas power plants during TexAQS 2000 and 2006, J. Geophys. Res.-Atmos., 115, D16303, doi:10.1029/2009jd013527, 2010.

Pickett-Heaps, C. A., Jacob, D. J., Wecht, K. J., Kort, E. A., Wofsy, S. C., Diskin, G. S., Worthy, D. E. J., Kaplan, J. O., Bey, I., and Drevet, J.: Magnitude and seasonality of wetland methane emissions from the Hudson Bay Lowlands (Canada), Atmos. Chem. Phys., 11, 3773–3779, doi:10.5194/acp-11-3773-2011, 2011.

Rigby, M., Prinn, R. G., Fraser, P. J., Simmonds, P. G., Langenfelds, R. L., Huang, J., Cunnold, D. M., Steele, L. P., Krummel, P. B., Weiss, R. F., O'Doherty, S., Salameh, P. K., Wang, H. J., Harth, C. M., Muehle, J., and Porter, L. W.: Renewed growth of atmospheric methane, Geophys. Res. Lett., 35, L22805, doi:10.1029/2008gl036037, 2008.

Rothman, L. S., Gordon, I. E., Barbe, A., Benner, D. C., Bernath, P. E., Birk, M., Boudon, V., Brown, L. R., Campargue, A., Champion, J. P., Chance, K., Coudert, L. H., Dana, V., Devi, V. M., Fally, S., Flaud, J. M., Gamache, R. R., Goldman, A., Jacquemart, D., Kleiner, I., Lacome, N., Lafferty, W. J., Mandin, J. Y., Massie, S. T., Mikhailenko, S. N., Miller, C. E., Moazzen-Ahmadi, N., Naumenko, O. V., Nikitin, A. V., Orphal, J., Perevalov, V. I., Perrin, A., Predoi-Cross, A., Rinsland, C. P., Rotger, M., Simeckova, M., Smith, M. A. H., Sung, K., Tashkun, S. A., Tennyson, J., Toth, R. A., Vandaele, A. C., and Vander Auwera, J.: The HITRAN 2008 molecular spectroscopic database, J. Quant. Spectrosc. Ra., 110, 533–572, doi:10.1016/j.jqsrt.2009.02.013, 2009.

Simpson, I. J., Rowland, F. S., Meinardi, S., and Blake, D. R.: Influence of biomass burning during recent fluctuations in the slow

growth of global tropospheric methane, Geophys. Res. Lett., 33, L22808, doi:10.1029/2006gl027330, 2006.

Simpson, I. J., Sulbaek Andersen, M. P., Meinardi, S., Bruhwiler, L., Blake, N. J., Helmig, D., Rowland, F. S., and Blake, D. R.: Long-term decline of global atmospheric ethane concentrations and implications for methane, Nature, 488, 490–494, doi:10.1038/nature11342, 2012.

Stephens, B. B., Gurney, K. R., Tans, P. P., Sweeney, C., Peters, W., Bruhwiler, L., Ciais, P., Ramonet, M., Bousquet, P., Nakazawa, T., Aoki, S., Machida, T., Inoue, G., Vinnichenko, N., Lloyd, J., Jordan, A., Heimann, M., Shibistova, O., Langenfelds, R. L., Steele, L. P., Francey, R. J., and Denning, A. S.: Weak northern and strong tropical land carbon uptake from vertical profiles of atmospheric CO_2, Science, 316, 1732–1735, doi:10.1126/science.1137004, 2007.

Sturm, P., Leuenberger, M., Sirignano, C., Neubert, R. E. M., Meijer, H. A. J., Langenfelds, R., Brand, W. A., and Tohjima, Y.: Permeation of atmospheric gases through polymer O-rings used in flasks for air sampling, J. Geophys. Res.-Atmos., 109, D04309, doi:10.1029/2003jd004073, 2004.

Tohjima, Y., Katsumata, K., Morino, I., Mukai, H., Machida, T., Akama, I., Amari, T., and Tsunogai, U.: Theoretical and experimental evaluation of the isotope effect of NDIR analyzer on atmospheric CO_2 measurement, J. Geophys. Res.-Atmos., 114, D13302, doi:10.1029/2009jd011734, 2009.

Tuzson, B., Hiller, R. V., Zeyer, K., Eugster, W., Neftel, A., Ammann, C., and Emmenegger, L.: Field intercomparison of two optical analyzers for CH_4 eddy covariance flux measurements, Atmos. Meas. Tech., 3, 1519–1531, doi:10.5194/amt-3-1519-2010, 2010.

Vay, S. A., Anderson, B. E., Conway, T. J., Sachse, G. W., Collins, J. E., Blake, D. R., and Westberg, D. J.: Airborne observations of the tropospheric CO_2 distribution and its controlling factors over the South Pacific Basin, J. Geophys. Res.-Atmos., 104, 5663–5676, doi:10.1029/98jd01420, 1999.

Wang, J. S., Logan, J. A., McElroy, M. B., Duncan, B. N., Megretskaia, I. A., and Yantosca, R. M.: A 3-D model analysis of the slowdown and interannual variability in the methane growth rate from 1988 to 1997, Global Biogeochem. Cy., 18, Gb3011, doi:10.1029/2003gb002180, 2004.

Washenfelder, R. A., Toon, G. C., Blavier, J. F., Yang, Z., Allen, N. T., Wennberg, P. O., Vay, S. A., Matross, D. M., and Daube, B. C.: Carbon dioxide column abundances at the Wisconsin Tall Tower site, J. Geophys. Res.-Atmos., 111, D22305, doi:10.1029/2006jd007154, 2006.

Wecht, K. J., Jacob, D. J., Wofsy, S. C., Kort, E. A., Worden, J. R., Kulawik, S. S., Henze, D. K., Kopacz, M., and Payne, V. H.: Validation of TES methane with HIPPO aircraft observations: implications for inverse modeling of methane sources, Atmos. Chem. Phys., 12, 1823–1832, doi:10.5194/acp-12-1823-2012, 2012.

Werle, P., Mucke, R., and Slemr, F.: The limits of signal averaging in atmospheric trace-gas monitoring by tunable diode-laser absorption spectroscopy (TDLAS), Appl. Phys. B, 57, 131–139, doi:10.1007/BF00425997, 1993.

Wilson, P. A., Manning, A. C., Macdonald, A. J., Etchells, A. J., and Kozlova, E. A.: Greenhouse gas measurement capability at the Carbon Related Atmospheric Measurement (CRAM) Laboratory at the University of East Anglia, United Kingdom, 15th WMO/IAEA Meeting of Experts on Carbon Dioxide, Other Greenhouse Gases and Related Tracers Measurement Techniques, Jena, Germany, 2009.

WMO: 14th WMO/IAEA Meeting of Experts on Carbon Dioxide Concentration and Related Tracers Measurement Techniques, Helsinki, Finland, 2007.

Wofsy, S. C. and The HIPPO Science Team and Cooperating Modellers and Satellite Teams: HIAPER Pole-to-Pole Observations (HIPPO): fine-grained, global-scale measurements of climatically important atmospheric gases and aerosols, Philos. T. Roy. Soc. A, 369, 2073–2086, doi:10.1098/rsta.2010.0313, 2011.

Wunch, D., Toon, G. C., Wennberg, P. O., Wofsy, S. C., Stephens, B. B., Fischer, M. L., Uchino, O., Abshire, J. B., Bernath, P., Biraud, S. C., Blavier, J.-F. L., Boone, C., Bowman, K. P., Browell, E. V., Campos, T., Connor, B. J., Daube, B. C., Deutscher, N. M., Diao, M., Elkins, J. W., Gerbig, C., Gottlieb, E., Griffith, D. W. T., Hurst, D. F., Jiménez, R., Keppel-Aleks, G., Kort, E. A., Macatangay, R., Machida, T., Matsueda, H., Moore, F., Morino, I., Park, S., Robinson, J., Roehl, C. M., Sawa, Y., Sherlock, V., Sweeney, C., Tanaka, T., and Zondlo, M. A.: Calibration of the Total Carbon Column Observing Network using aircraft profile data, Atmos. Meas. Tech., 3, 1351–1362, doi:10.5194/amt-3-1351-2010, 2010.

Yokelson, R. J., Goode, J. G., Ward, D. E., Susott, R. A., Babbitt, R. E., Wade, D. D., Bertschi, I., Griffith, D. W. T., and Hao, W. M.: Emissions of formaldehyde, acetic acid, methanol, and other trace gases from biomass fires in North Carolina measured by airborne Fourier transform infrared spectroscopy, J. Geophys. Res.-Atmos., 104, 30109–30125, doi:10.1029/1999jd900817, 1999.

Zhao, C. L. and Tans, P. P.: Estimating uncertainty of the WMO mole fraction scale for carbon dioxide in air, J. Geophys. Res.-Atmos., 111, D08s09, doi:10.1029/2005jd006003, 2006.